International Tables for Crystallography (2018). Vol. H, Section 2.8.2, pp. 174–177.

2.8. Powder diffraction in external electric and magnetic fields

H. Ehrenberg, M. Hinterstein, A. Senyshyn and H. Fuess

2.8.1. Introduction

The functionality of materials depends strongly on the crystalline structure and structural changes during operation. The term 'structure' usually refers to the ideal structure, which specifies the positions of the atoms in a lattice, and thus the distances and angles between them. This idealized model is, however, far too simple to describe the full functionality of a material in a device. Many types of defects, such as point defects, dislocations or grain boundaries, are essential to the functionality and have to be taken into account. As the length scales of defects range from atomic bond lengths *via* nanometres to micrometres, different methods have to be used for comprehensive structural characterization. High-resolution transmission electron microscopy (HRTEM) is the ideal tool for studying a material at the atomic scale, as it gives direct evidence of the arrangement of atoms. In addition, information on the chemical composition can be provided through X-ray or electron spectroscopies. However, in many cases electron microscopy requires a tremendous effort in sample preparation. Furthermore, the application of electric fields in a TEM column is a serious challenge with significant limitations. While electron microscopy will provide information on small sample volumes, diffraction methods probe larger quantities of samples, but give average information. In general, diffraction methods are based on electromagnetic or particle waves. X-ray photons with energies in the keV range have wavelengths similar to interatomic distances and, therefore, X-rays from laboratory sources or synchrotrons are the most widely used. Thermal neutrons with meV energies have complementary properties suited for other applications. While electrons are usually used for microscopy techniques, the field of electron crystallography has developed in recent years. However, given the very small size of an electron beam, its short wavelength (*circa* 0.03 Å) and high absorption, most particles studied by electron crystallography can be considered as single crystals. The combination of electron crystallography and powder diffraction is a powerful tool for tiny crystalline samples, especially inclusions (Weirich *et al.*, 2006).

In the field of *in situ* materials research, multiparametric measurements as functions of three or more external parameters, *e.g.* temperature–magnetic field–pressure or temperature–magnetic field–electric field, have been reported. However, the majority of so-called *in situ* studies are carried out as a function of temperature and sometimes of external pressure. Studies of structural changes under electric fields are relatively rare. Studies of changes due to magnetic fields almost entirely lie in the domain of neutron scattering, where single-crystal experiments usually give more details on the evolution of the magnetic structure. The challenges, necessary instrumentation and some examples of *in situ* diffraction measurements are described in Chapter 16 of the book *Modern Diffraction Methods* (Mittemeijer & Welzel, 2012).

2.8.2. Experimental conditions

Several challenges have to be overcome for experiments under external fields, so the exerimental conditions have to be adapted accordingly. As all these experiments are based on time-dependent conditions, the first requirement is a detecting system that allows fast data acquisition. Considerable progress in recent years has made time resolution of the order of nanoseconds possible (Schmitt *et al.*, 2007), thus enabling stroboscopic diffraction experiments. Higher time resolutions are possible with careful synchronization of the experiment with the time structure of a synchrotron X-ray beam. The electron bunches in a synchrotron are usually separated by several tens to hundreds of nanoseconds and have a width in the range of picoseconds. Once the gating window of an experiment is smaller than the time between successive bunches, the time resolution immediately reaches the width of a bunch. Structural responses to external stimuli are related to displacements of atoms and changes in unit-cell distortion (*i.e.* lattice parameters). The displacements are fairly small and thus very high sensitivity is a prerequisite. In order to study small unit-cell distortions, very good angular resolution is mandatory. The potential angular resolution that is possible in synchrotron experiments is very often not reached for powder samples, as the half-widths of the reflections are mainly determined by the microstructure.

In monochromatic neutron diffraction, the greater divergence of a neutron beam compared to a synchrotron beam and its spectral width ($\Delta\lambda/\lambda$) usually only allow a resolution in the range $\Delta d/d \simeq 10^{-2}$ to be achieved with medium-resolution (high-intensity) diffractometers; this can be tuned down to $\Delta d/d \simeq 10^{-3}$ by tightening the beam collimation at high-resolution monochromatic instruments. Significantly better resolution of $\Delta d/d \simeq 4 \times 10^{-4}$ can be achieved by combining the neutron time-of-flight technique with long neutron flight paths (*circa* 100 m) in back-scattering geometry. Even higher $\Delta d/d$ values (potentially down to 10^{-6}) can be obtained using the spin-echo-based neutron-scattering technique called Larmor diffraction (Repper *et al.*, 2009). The advantages of neutrons over X-rays are that they penetrate more deeply through materials, their scattering form factors are nearly independent of momentum transfer, and they are sensitive to the isotopic composition of a material, enabling accurate location of light elements in the presence of heavy ones, as well as the ability to distinguish between neighbouring elements in the periodic table. Whereas both synchrotron radiation and neutron scattering may be used to elucidate crystal structures under an electric field, neutrons can also be used to study magnetic order and its modification under a magnetic field. Therefore, the examples listed here for studies under electric fields use both kinds of radiation, whereas the examples of studies involving magnetic fields mainly use neutron scattering.

The properties of the materials discussed in this chapter are intimately related to their crystal structures; hence, any change in crystal structure is immediately reflected in the properties. The examples we have chosen are dominated by ferroelectric ceramics and lithium-ion battery materials on the one hand and multiferroic materials on the other.

Most reports in the literature on *in situ* or *in operando* studies deal either with the kinetics of chemical reactions (intercalation, crystallization, catalysis) or structural changes of materials under varying external conditions (temperature, pressure *etc.*). This

chapter is devoted to structural modifications under external fields, both electric and magnetic. The application of external fields requires dedicated sample environments; these often result in an increase in absorption and contribute to the scattering. Furthermore, some components of the devices used for these studies can cause inhomogeneity in the sample or texture. Challenges can be presented by, for example, the deposition of metallic contacts on ferroelectric ceramics, the pronounced materials interaction and mass transport accompanied by changes in electrode volumes in Li-ion batteries, and the housing of magnets.

2.8.2.1. *Detectors*

For an *in situ* or *in operando* study, the choice of detector depends on the specific demands of the study with respect to angular resolution and speed of data collection. High angular resolution is needed to investigate small changes in reflection profiles, resulting from tiny modifications in the microstructure. Fast data collection is generally desirable, but is particularly important when monitoring metastable states in fast and irreversible processes. For a general overview of commonly used X-ray detector systems see Chapter 2.1. The following is a detailed overview of detector systems with high angular or time resolution for X-ray as well as neutron powder diffraction.

For synchrotron X-ray diffraction, analyser crystals between the sample and detector allow angular resolutions to be achieved at the physical limit. Detection is performed point by point, or with a set of point detectors in a multi-analyser crystal detector (MAD) (Toraya *et al.*, 1996; Hodeau *et al.*, 1998; Lee *et al.*, 2008; Peral *et al.*, 2011). The angular resolution of these detectors is only limited by the Darwin width of the analyser crystals, the energy bandwidth of the monochromator and the divergence of the incoming beam.

Gas counters or neutron scintillators are usually used for the detection of thermal neutrons. Because of the shortage of ^{3}He for research applications, alternative technologies are undergoing rapid development, including ^{10}B-based detectors such as Cascade (Köhli *et al.*, 2016), Jalousie (Stefanescu *et al.*, 2017) and Multigrid (Anastasopoulos *et al.*, 2017). However, owing to their relatively low efficiency for thermal neutrons compared with ^{3}He gas counters, neutron detectors that involve $^{10}B(n,\alpha)^7Li$ conversion are mainly used for neutron non-diffraction applications. Even though an analyser setup would in theory be possible for neutron diffraction experiments, the drastically increased time that would be required for data acquisition means that it is not feasible. Alternative concepts have evolved for the use of monochromatic neutrons in powder diffraction with high angular resolution. Multidetectors consist of 80 (SPODI, Hoelzel *et al.*, 2007) or 128 (ECHIDNA, Liss *et al.*, 2006; D2B, Suard & Hewat, 2001) detection units [1/3, 1/2 or 1 inch (where 1 inch = 2.54 cm) diameter ^{3}He tubes, either position-sensitive or not] separated by a small angle and with Soller collimators installed in front. This requires a stepwise re-positioning of the detector bank in order to collect data for complete patterns. The angular resolution of these instruments is limited by the beam divergence, the energy bandwidth of the monochromator and grain-size effects (Liss *et al.*, 2006). A reduction in the divergence of a neutron beam is associated with a considerable loss of intensity. The prerequisites of low divergence and high take-off angle of the monochromator have to be optimized in combination with a two-dimensional detector system. The height of the detectors is limited, however, by the 'umbrella' effect, which produces a broadening of the Debye–Scherrer rings. This effect may be partially compensated for during the numerical data-reduction process (Hoelzel *et al.*, 2012). On the other hand, the detection of some extended sections of the Debye–Scherrer rings provides additional information on strain and texturing.

For a compromise of high angular resolution and fast data acquisition, one-dimensional strip detectors have become popular. These detectors allow data collection in one shot and thus no re-positioning is required. However, if more than one module is used, the gaps between the modules have to be filled by measuring two different positions. Silicon microstrip sensors are used for detecting X-rays (Bergamaschi *et al.*, 2009). The MYTHEN II detector system consists of a set of modules, each consisting of 1280 50 μm-pitch strips, which are wirebonded to the photon-counting readout (Bergamaschi *et al.*, 2009). In combination with a set of vertically focusing mirrors and a sagittally focusing second monochromator crystal, high angular resolution can be achieved together with short acquisition times (for example at the materials science beamline X04SA at the Swiss Light Source) (Patterson *et al.*, 2005). In order to cope with instantaneous many-photon deposition, which is typical of X-ray free-electron lasers (XFELs), a similar system based on the charge-integration principle has been developed (GOTTHARD, Cartier *et al.*, 2014).

For detecting neutrons, microstrip detectors are used, which consist of thin-film metallic strips of anodes and cathodes, deposited on electrically conducting Fe-containing 'black' glass in a ^{3}He gas chamber (*e.g.* D20, Hansen *et al.*, 2008). Similar specifications can be realized with a multiwire setup in ^{3}He gas chambers (WOMBAT, Studer *et al.*, 2006). The multiwire detector has the advantage of being fully two-dimensionally sensitive. This allows for a larger aperture along the wires. The angular resolution can be maintained in the data-reduction process through straightening of the Debye–Scherrer rings. As Soller collimators cannot be used in front of a multiwire or multistrip detector, the effects of sample environments are eliminated by radial oscillating collimators. Multiwire and multistrip detectors are usually installed at high-throughput instruments, whereas high-resolution powder diffractometers are equipped with multidetector systems.

In materials science the investigation of real structure effects can be important. These can include texturing, where the orientation of the sample with respect to the scattering vector is crucial, or diffuse scattering in crystalline materials, and where a large dynamic intensity range has to be covered. The most efficient way of detecting these effects is to use two-dimensional detectors. In most cases the detector is mounted on a set of translational stages, so that the setup can be optimized for either high angular resolution or a wide angular range (Herklotz *et al.*, 2013).

When high-energy X-rays are used, two-dimensional detectors based on digital flat-panel technology are the best choice. They combine an amorphous Si panel with a CsI:Tl or various Gd_2O_2S:Tb scintillators. Pixel sizes of 200 × 200 μm (Perkin Elmer 1621N ES, Herklotz *et al.*, 2013) or 154 × 154 μm (Pixium 4700, Daniels & Drakopoulos, 2009) together with frame rates of up to 60 frames per second overcome several drawbacks of the high-energy detectors that were previously available.

For soft X-rays a range of two-dimensional detectors has been developed. The PILATUS detector (Kraft *et al.*, 2009) is a silicon-based hybrid pixel detector system, similar to the MYTHEN strip detector. Instead of a one-dimensional strip setup, individual modules with 487 × 195 pixels of identical pitch (172 × 172 μm)

are combined into a detector array of up to 6 224 001 pixels. A further development of the PILATUS detector is the EIGER detector (Johnson *et al.*, 2014). The system consists of single-photon-counting modules of 256 × 256 pixels with a significantly reduced pitch of only 75 × 75 μm. Like GOTTHARD, the charge-integrating equivalent of MYTHEN, the JUNGFRAU detector (Mozzanica *et al.*, 2014) was developed as a charge-integrating equivalent to the PILATUS and EIGER detectors.

Even smaller pixel sizes of 55 × 55 μm have been achieved for the hybrid pixel detector Medipix3 (Ballabriga *et al.*, 2007). Modules of 256 × 256 pixels can be combined into large arrays. The electronics are highly configurable and allow charge summing, programmable binary counter and continuous count–read modes.

In principle, fast data collection seems to be desirable, but it has to be adjusted to the process that is being investigated. In most cases for a continuous frame rate the limiting factor is the data rate. The MYTHEN II detector (Schmitt *et al.*, 2003) installed at the Swiss Light Source allows a frame rate of 10–90 Hz, depending on the desired dynamic range (24–4 bits), and thus observations in the time range below 1 s to 10 ms. The two-dimensional detectors for high-energy X-rays can operate at a maximum of 30 Hz (Perkin Elmer) or 60 Hz (Pixium). In this context it is also worth mentioning the PILATUS detectors – a series of silicon pixel detectors also developed at the Swiss Light Source and further commercialized by Dectris. These detectors possess a high dynamic range over five orders of magnitude along with a rate capability of $>2 \times 10^6$ photons s^{-1} $pixel^{-1}$ and excellent detection efficiency of nearly single-photon counting (99% at 8 keV and 55% at 15 keV). The use of 1000 μm-thick CdTe instead of silicon enables >90% quantum efficiency at 20 keV, 81% at 40 keV, 90% at 60 keV, 77% at 80 keV and 56% at 100 keV. Complex detectors are often characterized by a long readout time of a large number of two-dimensional pixels, *e.g.* for PILATUS detectors the readout time per module is ∼2.7 ms.

Semiconductor-based detectors can operate at significantly higher frame rates. The EIGER detector can operate at a maximum frame rate of 24 kHz, while GOTTHARD can reach 40 kHz. In a special burst mode of 128 frames, a frame rate of 800 kHz is possible, reaching a single exposure time of 1.25 μs. The Timepix3 detector (Poikela *et al.*, 2014), which is a further development of the Medipix3 detector, can theoretically sustain continuous frame rates of up to 200 kHz, as long as the overall hit rate is less than 80 MHz.

In order to collect enough intensity for fast processes or to investigate even shorter timescales, stroboscopic measurements are useful. Thus, timescales in the range of milliseconds down to nanoseconds may be followed using a pump–probe setup. In this technique, the reaction is first triggered (pump) and after a specific time delay the diffraction pattern is collected (probed). The use of rapidly rotating choppers in the incoming beam is an attractive alternative to pump–probe experiments (Yoo *et al.*, 2011). Time resolution in the microsecond regime is routinely obtained in synchrotron experiments (Hinterstein, 2011; Hinterstein *et al.*, 2014) and in about the millisecond regime in neutron diffraction (Eckold *et al.*, 2010). When these experiments are conducted at a synchrotron and the periodic excitation of the sample is synchronized with the bunch clock of the synchrotron, the time resolution can be increased significantly. For a time resolution smaller than the temporal separation of the particle bunches (typically 8–200 ns), the time resolution suddenly drops to the bunch width, which is in the range of picoseconds. For neutron diffraction, the limiting factor for time resolution can be calculated from the energy bandwidth and the speed of the neutrons, which is dependent on the wavelength. The lower limit is typically in the range of 25 μs. These time ranges can be reached by multistrip or multiwire detectors in a stroboscopic setup.

In situ and *in operando* measurements require a specific sample environment, which is normally built using a different material to the sample and leads to additional contributions to the diffraction pattern. The use of strongly scattering materials such as thin metallic foils (Al foil in batteries, Ag or Au films as electrodes) or single crystals (sapphire capillaries for high-temperature experiments or diamonds in high-pressure experiments) may seriously bias data collection or damage the detector. If it is not possible to eliminate them by masking, they have to be taken into account by Rietveld analysis or profile matching. A correct treatment of the contributions from the sample environment has to take into consideration the fact that the additional scattering is normally off the diffractometer centre and this sample shift produces a non-linear shift in 2θ of the corresponding reflections in the pattern.

2.8.2.2. *Absorption*

Additional equipment is required for *in situ* experiments. The necessary parts are quite often constructed from metallic components. Light metals like aluminium are preferred for shielding parts within the beam for neutrons and X-rays. Vanadium is a suitable choice in neutron experiments, as it has a very small scattering cross section, so produces almost no coherent scattering. In most cases a suitable absorption correction is mandatory. For X-rays the energy dependence of the linear absorption coefficient $\mu(E)$ is very pronounced, especially close to X-ray absorption edges. Away from an absorption edge, higher energies lead to lower absorption. As an example, the linear absorption coefficient μ for steel (α-Fe) at 45 keV is 0.18 cm^{-1} and at 60 keV it is 0.076 cm^{-1}. The transmitted intensity after a beam has penetrated 1 mm steel with 100% packing density twice (once for the incoming and once for the outgoing beam) is therefore 2.7% for 45 keV but 22% for 60 keV. For one of the examples treated later, the piezoceramic $Pb(Zr_{0.5}Ti_{0.5})O_3$, the calculation for a sample diameter of 1 mm and a typical packing density of 60% in a powder leads to beam transmission of 3% (45 keV) and 21% (60 keV). Therefore, using high-energy X-rays enables transmission diffraction experiments that are not feasible with lower energies. The gain in measured intensities by decreasing absorption normally overcompensates for the decrease in scattering at shorter wavelengths, which is proportional to λ^3 within kinematical theory. The linear absorption coefficient of thermal neutrons (with wavelengths from 1 to about 3 Å) is small for most elements and scales in proportion to the wavelength, $\lambda = h/p = h/(2mE)^{1/2}$, *i.e.* λ (Å) = $9.045/E^{1/2}$ (meV) = $3956/v$ (m s^{-1}). However, the absorption cross sections for different isotopes of the same element may be very different. Numerical values are listed in Sears (1992) and *International Tables for Crystallography* Volume C, Table 4.4.4.1. For ferroelectric $Pb(Zr_{0.5}Ti_{0.5})O_3$, the linear neutron absorption coefficient at a wavelength λ = 1.5 Å and for a packing density of 60% is 0.026 cm^{-1}, significantly smaller than for X-rays; it is mainly determined by the Ti content.

As both the scattering and the absorption cross section for neutrons are in most cases much smaller than for X-rays, bigger samples are required. On the one hand, this leads to the advantage of better averaging over many particles. On the other hand,

the spatial resolution is significantly affected by the sample dimensions because of self-collimation. The appropriate choice of diffraction method is defined by the particular scientific challenge and has to take into consideration the different amount of sample that is needed for each experiment.

Very high absorption cross sections are desirable for shielding purposes. In X-ray diffraction, lead or tungsten are widely used. Only a few isotopes have a nuclear resonance in the thermal neutron range and thus a high absorption cross section. The most prominent are ^{10}B, ^{113}Cd and ^{157}Gd, which are used in neutron optics as collimators, attenuators and beam-shaping devices.

2.8.2.3. *Sample fluorescence and incoherent neutron scattering*

Sample fluorescence is a common problem for laboratory X-ray powder diffractometers, which are neither equipped with an analyser nor use detectors with a narrow energy resolution. In powder diffraction using synchrotron radiation, this problem is often solved either by adjusting the energy of the incident beam or by an adjustment of the dynamic range of the detector, or by a combination of both.

Like absorption cross sections, the incoherent neutron scattering lengths for different elements and isotopes do not vary in any obviously systematic way throughout the periodic table. Among the known stable isotopes, ^{1}H has the largest incoherent scattering length (25.274 fm) and has a small and negative coherent one (−3.7406 fm). The situation is very different for ^{2}H (deuterium), for which the incoherent and coherent scattering lengths are 4.04 and 6.671 fm, respectively. Differences between the coherent scattering lengths of hydrogen and deuterium form the basis of the isotopic labelling technique, called contrast matching; this is particularly important in applications of neutron scattering to hydrogen storage, structural biology and polymer science. Deuteration of samples is a challenging task, but obtaining high-quality powder diffraction data from hydrogenated samples is far more difficult. Use of neutron polarization analysis is a reliable way to subtract the incoherent scattering contribution from the diffraction data (Mikhailova *et al.*, 2012), but it is often accompanied by significant losses of incident neutron flux and, consequently, of data quality. Both sample fluorescence and incoherent neutron scattering are isotropic and, therefore, are often considered as a background in powder diffraction experiments.

2.8.3. Examples

2.8.3.1. *In situ studies of ferroelectrics in an external electric field*

The function of ferroelectrics as stress sensors, high-frequency microphones, medical injectors or large strain actuators is based on electric poling. A polycrystalline material exhibits a zero net polarization. When an electric field is applied to the sample, the spontaneous electric polarization of the ferroelectric material is reoriented along the electric field vector. This occurs by a reorientation of domains. Additional polarization is obtained by an increase of the spontaneous polarization induced by the applied electric field. With *in situ* experiments, the field-induced changes in the powder diffraction reflections are measured. Fig. 2.8.1 is a schematic representation of some *in situ* sample geometries. The electric field is applied *via* electrodes on the sample surface.

Many of these ferroelectric materials crystallize in a structure derived from the cubic perovskite type, but in a crystal system with lower symmetry and with a non-centrosymmetric space group. The most widely used material is lead zirconate-titanate ($PbZr_{1-x}Ti_xO_3$, PZT), which exhibits the highest strain response

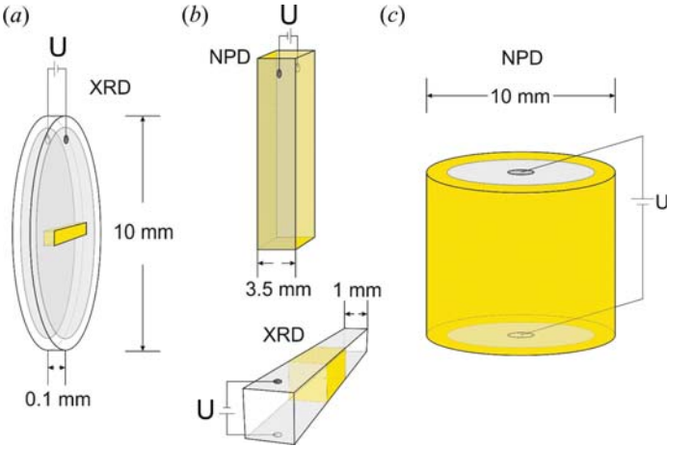

Figure 2.8.1
Sample geometries for *in situ* experiments with an applied electric field. Samples are poled *via* an applied voltage (U) at the sample electrodes (grey). Different sample geometries are necessary to account for different beam sizes, absorption and detector concepts. Yellow indicates the irradiated sample volume. (*a*) Flat-plate samples for X-ray experiments with strip detectors, limiting photon energies to around 30 keV. (*b*) Bar-shaped samples for high-intensity neutron powder diffraction (NPD) or high-energy X-ray diffraction (XRD). (*c*) Cylinder-shaped samples for high-resolution neutron diffraction with fixed detector collimators.

at the so-called morphotropic phase boundary with a composition of about 50% for Ti and Zr. It is generally accepted that the phase on the Ti-rich side of the PZT phase diagram has a tetragonal structure with space group *P*4*mm*. On the rhombohedral Zr-rich side, two ferroelectric phases can be identified, with space groups *R*3*m* for high and *R*3*c* for low temperatures. A considerable amount of work has been devoted to the elucidation of the crystal structure of the material close to the morphotropic phase boundary. Neutron and synchrotron diffraction detected monoclinic symmetry at low temperatures and nanometre-sized regions (the so-called polar nanoregions) were inferred from diffuse scattering (Noheda *et al.*, 2000; Hirota *et al.*, 2006). Alternative interpretations explained the new reflection found in the pattern between the 111_C and 200_C reflections (where the subscript 'C' corresponds to the cubic archetype structure) as diffuse scattering from diffuse incoherent scattering by small domains (Jin *et al.*, 2003).

Unique information on structural changes during poling is obtained from *in situ* studies in applied external electric fields (Hoffmann *et al.*, 2001). Fig. 2.8.2 displays two groups of powder reflections (Schönau, Schmitt *et al.*, 2007) observed by synchrotron X-ray diffraction. They are directly compared with the domain structure from TEM observations (Schmitt *et al.*, 2007) for a range of compositions near the morphotropic phase boundary. One group of reflections is derived from the cubic 111_C reflection, the other from the archetype 200_C reflection. The transition from the rhombohedral splitting to the tetragonal one with increasing Zr content is correlated with the forms of ferroelectric domains in TEM. Close to the morphotropic phase boundary, nanodomains (ranging in width from 20 to 200 nm) are observed in addition to the well known microdomains. The nanodomains react immediately under the influence of an electric field to become microdomains. Fig. 2.8.3 shows the intensity changes observed for the 110_C group of reflections. The changes under an electric field are pronounced and depend on the *c*/*a* ratio (Schönau, Knapp *et al.*, 2007), the formation and disappearance of nanodomains, and the local symmetry of these domains.

references